The Journal of Veterinary Medical Science

NOTE

Pathology

An aortic body carcinoma with sarcomatoid morphology and chondroid metaplasia in a French Bulldog

Chiaki MORITA[1)], Miyuu TANAKA[2)], Shunsuke NOGUCHI[2)], Shunsuke SHIMAMURA[2)], Yusuke WADA[2)], Takeshi IZAWA[1)], Jyoji YAMATE[1)] and Mitsuru KUWAMURA[1)]*

[1)]Laboratory of Veterinary Pathology, Graduate School of Life and Environmental Sciences, Osaka Prefecture University, Izumisano, Osaka 598-8531, Japan
[2)]Veterinary Medical Center, Osaka Prefecture University, Izumisano, Osaka 598-8531, Japan

J. Vet. Med. Sci.
82(5): 576–579, 2020
doi: 10.1292/jvms.20-0016

Received: 8 January 2020
Accepted: 28 February 2020
Advanced Epub:
12 March 2020

ABSTRACT. An 11-year-old female French Bulldog was presented with a mass at the base of the heart, detected by X-ray and echocardiography. Clinical abnormality included abdominal retention by ascites. Radiation therapy was performed for 5 weeks. The mass volume didn't change during the radiotherapy. The condition became worse and the dog died 6 months after the initial presentation and necropsy was performed. Grossly, the mass, 12.5 × 6.5 × 6.0 cm in size, was found at the base of the heart. Histopathological examination revealed that cardiac mass was composed of alveolar, bundle and diffuse proliferation of neoplastic cells. Most of the neoplastic cells showed a spindle morphology; in some areas small round or polyhedral neoplastic cells were observed. Occasional cartilage metaplasia was seen multifocal in the mass, and it was surrounded by the sarcomatoid proliferation. Electron microscopy revealed a few neuroendocrine granules in the cytoplasm of spindle and polyhedral neoplastic cells. Metastatic cells in the lungs which had not irradiated demonstrated typical morphology of aortic body tumors. Based on these findings, the case was diagnosed as an aortic body carcinoma with sarcomatoid morphology and chondroid metaplasia.

KEY WORDS: aortic body carcinoma, dog, sarcomatous transformation

An aortic body is a chemoreceptor organ located in the periadventitial tissue near the base of the heart, which detects hypoxemia and changes the regulation of respiration and circulation by peripheral nerves [10, 11]. It is composed of polyhedral-shaped chemoreceptor and stellate-shaped sustentacular cells [11]. Chemodectomas develop primarily in dogs especially brachycephalic breeds such as boxer and Boston terrier [12]. Genetic predisposition and chronic hypoxia may account for the higher risk of chemodectomas [12]. Although it is considered that canine aortic body carcinomas occur less frequently than adenomas, there are reports that canine aortic body tumors are considered to be potentially malignant [12, 15]. Aortic body tumor cells often invade blood vessels and infrequently metastasis to the lungs, liver, or bones in dogs [3, 5, 12]. Aortic body tumors usually consist of sheets or clusters of polyhedral cells with eosinophilic granular cytoplasm, separated by fine fibrous stroma [11]. To our knowledge, there is no report of canine aortic body carcinoma with sarcomatoid morphology and chondroid metaplasia. Here we describe the first case of canine aortic body carcinoma with sarcomatoid morphology.

An 11-year-old female French Bulldog was presented to a private animal clinic with abdominal distension. A mass at the base of the heart was detected by X-ray and echocardiography. The dog was referred to the Veterinary Medical Center, Osaka Prefecture University one week after the initial presentation. Computed tomography revealed a mass with soft tissue density at the dorsal part of the heart base. The dog had abdominal retention by ascites and swelling of mediastinal and parasternal lymph nodes was found. Fine needle aspiration from the mediastinal lymph node was conducted and malignant epithelial tumor, especially metastatic chemodectoma was suspected. Radiation therapy was performed for 5 weeks (6 Gy par time; total 36 Gy) by using 4 MV X-ray linear accelerator (PRIMUS; Toshiba Medical Systems Corp., Otawara, Japan) from 12 days after the initial presentation. The mass volume didn't change during the radiotherapy. The ascites retention improved transiently, however, recurred 4 months after the initial presentation. The condition became worse and pulmonary edema was suspected on 6 months after the initial presentation. The dog then died and necropsy was performed.

*Correspondence to: Kuwamura, M.: kuwamura@vet.osakafu-u.ac.jp
(Supplementary material: refer to PMC https://www.ncbi.nlm.nih.gov/pmc/journals/2350/)

At necropsy, the mass was 12.5 × 6.5 × 6.0 cm in size and found at the base of the heart (Supplementary Fig. 1). The mass was solid and the cut surface was grayish. There were two small nodules of 0.6 cm in diameter in the dorsal part of right lung, and one nodule of 0.4 × 0.4 cm in diameter in the ventral part of left lung. Marked dilatation of the right ventricle and pericardial effusion (30 m*l*, diluted blood-like) were found. There was a chronic congestive liver with a nut-meg like appearance. Fibrinous deposition on the liver surface and accumulation of biliary sludge in the gall bladder were observed. Pleural effusion (300 m*l*, blood-like) and accumulation of ascites (160 m*l*, pink) were noted. Multifocal hemorrhage was found in the pancreas.

Tissue specimens were collected from the liver, spleen, kidneys, heart, lungs, stomach, small and large intestines, gall bladder, urinary bladder, and pancreas.

These samples were fixed in 10% neutral buffered formalin, processed routinely and embedded in paraffin wax. Sections at 5 μm were cut and stained with hematoxylin and eosin (HE). Sections were also subjected to immunohistochemistry (IHC) with primary antibodies specific for cytokeratin AE1/AE3, vimentin, chromogranin A, synaptophysin, S100 and α-smooth muscle actin (Supplementary Table 1). After dewaxing and pretreatment, tissue sections were processed in a Histostainer™ (Nichirei Biosciences, Tokyo, Japan). Sections were treated with 5% skimmed milk in phosphate buffered saline (PBS) for 15 min and reacted with each primary antibody for 1 hr. After incubation in 3% H_2O_2 for 15 min, application of horseradish peroxidase-conjugated secondary antibody (Histofine Simple Stain MAX PO®; Nichirei Biosciences) was performed for 1 hr. Positive reactions were visualized with 3, 3′-diaminobenzidine (DAB substrate kit; Nichirei Biosciences). Sections were counterstained lightly with hematoxylin. Formalin-fixed tissues were also fixed in 2.5% glutaraldehyde in 0.1 M phosphate buffer (PB; pH 7.4), post-fixed with 1% osmic tetraoxide at 4°C overnight, and embedded in epoxy resin. Ultrathin sections were stained with uranyl acetate and lead citrate and examined in a Hitachi H-7500 electron microscope (Hitachi, Tokyo, Japan).

Histopathological examination revealed that the cardiac mass was composed of alveolar, bundle and diffuse proliferation of neoplastic cells (Supplementary Fig. 2). Most of the neoplastic cells were spindle shaped (sarcomatoid) (Fig. 1A), and in some areas (approximately one fourth areas) small round or polyhedral neoplastic cells were arranged in nests separated by thin fibrous tissue (Fig. 1B). Morphological transition between spindle, round and polyhedral cells was found (Fig. 1A). The cytoplasm of neoplastic cells was lightly eosinophilic and finely granular. Neoplastic cells showed prominent cellular and nuclear atypia. Occasionally giant neoplastic cells with bizarre shaped nuclei were found. Mitotic figures were rarely seen (3 par 10 high-power [×400] fields). Occasional cartilage metaplasia was seen multifocally in the mass, surrounded by sarcomatoid proliferation (Fig. 2). The cartilagenous areas showed metachromasia with toluidine blue stain (Supplementary Fig. 3). Neoplastic cells invaded to ventricular septal and left ventricular myocardium. IHC revealed that small, round, polyhedral and giant shaped neoplastic cells were positive for synaptophysin (Fig. 3), vimentin, chromogranin A and cytokeratin AE1/AE3 (Fig. 4), while they were negative for S-100 and α-smooth muscle actin. Spindle shaped neoplastic cells were positive for vimentin, and chromogranin A, while they were negative for AE1/AE3, synaptophysin, S-100 and α-smooth muscle actin. Cartilages were positively stained with vimentin, very faintly stained with chromogranin A, whereas other IHCs were negative. Electron microscopy revealed that a few membrane-bounded neuroendocrine granules in the cytoplasm of spindle and polyhedral neoplastic cells (Supplementary Fig. 4). Neoplastic cells metastasized to the lungs were typical morphology of aortic body tumors (Supplementary Fig. 5).

Other histopathological findings, except for neoplastic lesions, was observed in the heart, liver, and pancreas. There was atrophy and vacuolar degeneration in the myocardium. Severe congestion and atrophy of hepatocytes was seen in the liver. In the pancreas, hemorrhage and necrosis was seen in the gross foci of hemorrhage.

In this case, the expansive mass at the heart base compressed the surrounding vessels and caused dilatation of right ventricle, and circulatory disturbance was considered to be the cause of death. Previous reports support that chromogranin A and synaptophysin are useful diagnostic makers for chemodectomas [1, 12, 14, 15]. In addition, membrane-bounded granules were found both in the spindle and polyhedral neoplastic cells. From these findings, we diagnosed this tumor as an aortic body carcinoma with sarcomatoid morphology and chondroid metaplasia.

Clear differentiation between benign and malignant aortic body tumors is not always possible. The most definitive criteria for malignancy are documented metastasis or invasion, grossly or microscopically [12]. We considered that the present case is malignant, because of metastasis to the lung and invasive growth to the myocardium. The present tumor had various cell morphology, showing spindle to polyhedral neoplastic cells. The neoplastic cells with different morphology showed the same immunophenotype and there was morphological transition between the spindle and polyhedral cells, we considered that all neoplastic cells with different morphology originated from a same tumor. This tumor had extensive sarcomatoid areas where spindle cells proliferated and occasional cartilage formation was found. Metastatic cells in the lungs which had not irradiated demonstrated typical morphology of aortic body tumors. It may be a possibility that morphological change of neoplastic cells in this tumor may be influenced by the effect of X-ray because radiation had applied locally to the base of the heart using a 4 MV X-ray linear accelerator.

In humans, sarcomatous transformation of epithelial tumor after irradiation was reported in several cases such as pituitary gland sarcoma [9, 13] and prostatic adenocarcinoma [2, 4]. The average dose of radiation in documented cases of post irradiation pituitary sarcoma was 42.3 Gy (24 Gy to 78 Gy) [9]. Precise effect of irradiation to the histopathological change was uncertain; the present case had total dose of 36 Gy radiation.

Cartilaginous formation was reported in several canine malignant melanoma [6, 8]. It is suggested that the cartilage matrixes are produced by dedifferentiated melanocytes [8]. Aortic body tumors are considered to be derived from cells of the neural crest [11], and same as melanocytes [7].

To the best of our knowledge, this is the first report of aortic body carcinoma with sarcomatoid morphology and chondroid metaplasia in a dog. Morphological effect to the neoplastic cells by local irradiation remains to be elucidated.

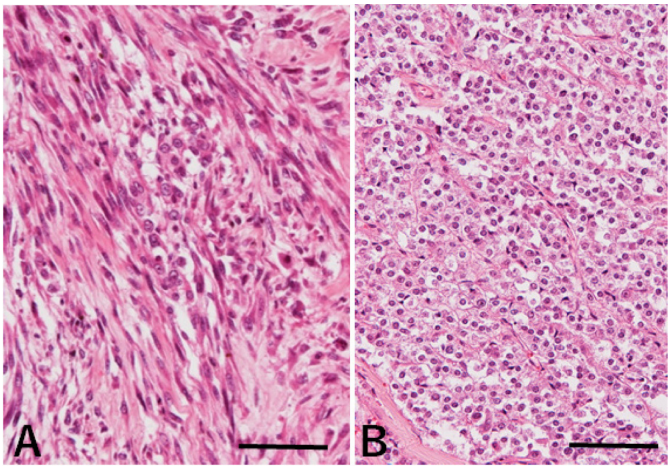

Fig. 1. Sarcomatoid proliferation of spindle shaped neoplastic cells (A) and small round neoplastic cells were arranged in nests (B). Small round tumor cells were found in the center of Fig. 1A and morphological transition between spindle and round cells is observed. Hematoxylin and Eosin stain (HE). Bars, 50 μm

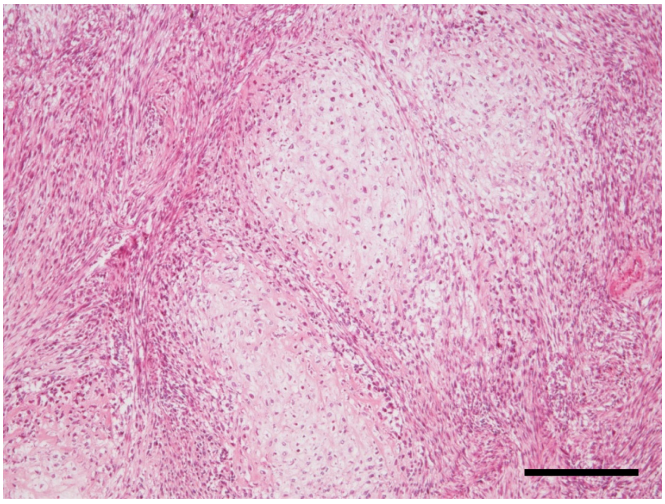

Fig. 2. Cartilage metaplasia is surrounded by sarcomatoid proliferation. Hematoxylin and Eosin stain (HE). Bar, 300 μm

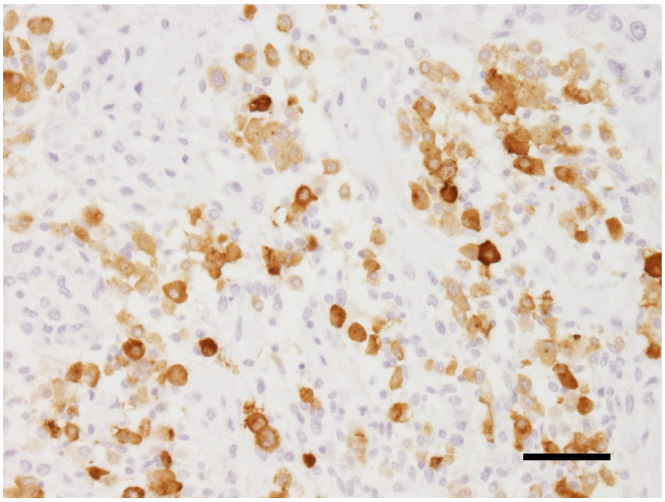

Fig. 3. Polygonal shaped neoplastic cells are positive for synaptophysin. The base of the heart mass. Immunohistochemistry counterstained with hematoxylin. Bar, 50 μm

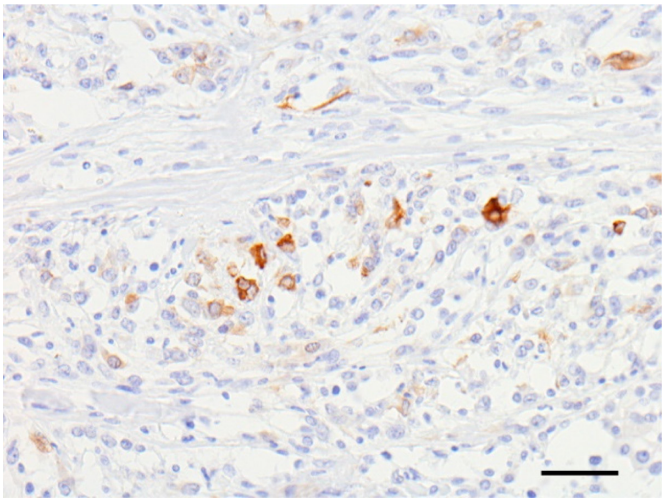

Fig. 4. Round or polyhedral shaped neoplastic cells are positive for cytokeratin AE1/AE3. The base of the heart mass. Immunohistochemistry counterstained with hematoxylin. Bar, 50 μm

REFERENCES

1. Brown, P. J., Rema, A. and Gartner, F. 2003. Immunohistochemical characteristics of canine aortic and carotid body tumours. *J. Vet. Med. A Physiol. Pathol. Clin. Med.* **50**: 140–144. [Medline] [CrossRef]
2. Dundore, P. A., Cheville, J. C., Nascimento, A. G., Farrow, G. M. and Bostwick, D. G. 1995. Carcinosarcoma of the prostate. Report of 21 cases. *Cancer* **76**: 1035–1042. [Medline] [CrossRef]
3. Gliatto, J. M., Crawford, M. A., Snider, T. G. 3rd. and Pechman, R. 1987. Multiple organ metastasis of an aortic body tumor in a boxer. *J. Am. Vet. Med. Assoc.* **191**: 1110–1112. [Medline]
4. Huan, Y., Idrees, M., Gribetz, M. E. and Unger, P. D. 2008. Sarcomatoid carcinoma after radiation treatment of prostatic adenocarcinoma. *Ann. Diagn. Pathol.* **12**: 142–145. [Medline] [CrossRef]
5. Kim, S. K., Hyun, C. B. and Cho, K. O. 2005. Unusual metastasis of malignant aortic body tumor to multiple bones in a dog. *J. Vet. Med. Sci.* **67**: 625–627. [Medline] [CrossRef]
6. Kuwamura, M., Ide, M., Kuribayashi, M., Yamate, J., Nomura, K. and Kotani, T. 2000. Malignant melanoma with cartilaginous formation in a dog. *J. Toxicol. Pathol.* **13**: 269–270. [CrossRef]

7. Mort, R. L., Jackson, I. J. and Patton, E. E. 2015. The melanocyte lineage in development and disease. *Development* **142**: 620–632. [Medline] [CrossRef]
8. Oyamada, T., Tanaka, H., Park, C. H., Ueki, H., Komiya, T. and Arai, S. 2007. Pathology of canine oral malignant melanoma with cartilage and/or osteoid formation. *J. Vet. Med. Sci.* **69**: 1155–1161. [Medline] [CrossRef]
9. Powell, H. C., Marshall, L. F. and Ignelzi, R. J. 1977. Post-irradiation pituitary sarcoma. *Acta Neuropathol.* **39**: 165–167. [Medline] [CrossRef]
10. Romanucci, M., Malatesta, D., Berardi, I., Pugliese, G., Fusco, D. and Della Salda, L. 2014. Cytological, histological and ultrastructural nuclear features of monster cells in a canine carotid body carcinoma. *J. Comp. Pathol.* **151**: 57–62. [Medline] [CrossRef]
11. Rosol, T. J. and Grone, A. 2015. Endocrine glands. pp. 269–357. *In*: Jubb, Kennedy, and Palmer's Pathology of Domestic Animals, 6th ed. (Maxie, m. G. ed.), Elsevier Saunders, Philadelphia.
12. Rosol, T. J. and Meuten, D. J. 2017. Tumors of the endocrine glands. pp. 766–833. *In*: Tumors in Domestic Animals (Meuten, D. J. ed.), 5th ed., Wiley Blackwell, Ames.
13. Sato, K., Hayashi, M., Komai, T., Kubota, T., Kawano, H. and Handa, Y. 1990. [Clinical and histological study of pituitary fibrosarcoma following radiotherapy for pituitary adenoma. Case report]. *Neurol. Med. Chir. (Tokyo)* **30**: 888–892 (in Japanese). [Medline] [CrossRef]
14. Teh, A. P., Pratakpiriya, W., Hidaka, Y., Sato, H., Hirai, T. and Yamaguchi, R. 2017. An atypical case of recurrent carotid body carcinoma in a young adult dog: Histopathological, immunohistochemical and electron microscopic study. *J. Vet. Med. Sci.* **79**: 714–718. [Medline] [CrossRef]
15. Yamamoto, S., Fukushima, R., Hirakawa, A., Abe, M., Kobayashi, M. and Machida, N. 2013. Histopathological and immunohistochemical evaluation of malignant potential in canine aortic body tumours. *J. Comp. Pathol.* **149**: 182–191. [Medline] [CrossRef]